ELSEVIER

Journal of Nuclear Materials 247 (1997) 265–272

journal of nuclear materials

Characteristic thermodynamic properties of $M_yU_{1-y}O_{2+x}$ ($M = M^{4+}$, M^{3+} and M^{2+}; $x \gtreqless 0$) solid solutions and the phase behavior of Mg solid solution in low oxygen pressures

Takeo Fujino *, Nobuaki Sato, Kohta Yamada

Institute for Advanced Materials Processing, Tohoku University, 2-1-1 Katahira, Aoba-ku, Sendai 980-77, Japan

Abstract

After a short review on the existing regions and thermodynamic properties of essentially ionic ternary uranium dioxide solid solutions, $M_yU_{1-y}O_{2+x}$ ($x \gtreqless 0$), classified by the valency of the M metals, a description is made for our study on the solubility and the crystal chemistry of Mg in the Mg solid solution in a range of low p_{O_2}. The single phase region extended up to at least $y = 0.1$ at 1200°C in $p_{O_2} = 10^{-15}$ or $\leq 10^{-19}$ atm. Density measurements revealed that the Mg atoms in the solid solution formed under the above conditions are about 60% in the interstitial sites. This experimental result was rationalized by the calculated $\Delta\overline{G}_{O_2}$ change caused from the configurational partial molar entropy obtained through the lattice statistics of the occupation of Mg and oxygen atoms in the solid solution lattice sites. © 1997 Elsevier Science B.V.

1. Introduction

Various kinds of fission product metals form solid solutions with UO_2 causing frequently a significant change in the thermodynamic properties of the fuel. Oxygen potentials in the presence of such metals have been measured for some idealized or simulated cases of irradiation [1–3].

On the other hand, the doping effect of a small amount of impurity metals into UO_2 has been studied in an effort to improve the fuel performance during irradiation. The metals which attracted attention are, for example, Mg [4], Ca + Ti [5], La [6], Cr [7], Ti, V and Nb [5,6,8]. However, the thermodynamic data of these doped fuel oxides are not sufficient. Thermodynamic consideration becomes more important as the doped metal concentration is higher (e.g., several wt% Gd content for burnable poison fuel [9,10]).

In this paper, after reviewing on the thermodynamic properties of $M_yU_{1-y}O_{2+x}$ ($x \gtreqless 0$) shortly, a study on the solubility of Mg in UO_2 in low oxygen pressures is described. Density measurements showed the existence of interstitial Mg atoms in the solid solution, which was analysed by lattice statistics of Mg and oxygen atoms in the different crystallographic sites as a function of oxygen potential.

2. A short review on the phase relations and oxygen potentials of solid solutions as classified by the valence of doped metals

2.1. Metals having +4 valence state

Due to the small crystal radius of Zr^{4+} [11], the solubility of ZrO_2 is low. The Zr solid solution, $Zr_yU_{1-y}O_{2+x}$ ($x \geq 0$), with $y = 0.1$–0.3 is considered to be metastable but it does not easily decompose by heating at around 1000°C [12,13]. ThO_2

* Corresponding author. Tel.: +81-22 217 5163; fax: +81-22 217 5164.

PII S0022-3115(97)00074-3

forms a solid solution with stoichiometric UO_2 in all ratios. However, with non-stoichiometric UO_{2+x}, the solid solution separates into two phases for a lower content of ThO_2 [14].

Similar to UO_{2+x}, the oxygen potential, $\Delta\overline{G}_{O_2} = RT \ln p_{O_2}$, of $M_yU_{1-y}O_{2+x}$ (M = Zr and Th) decreases steeply as x (> 0) decreases approaching to zero. However, in the effect of the metal addition there is a difference. While Th causes an increase in $\Delta\overline{G}_{O_2}$ [15], Zr decreases $\Delta\overline{G}_{O_2}$ [13]. According to Hoch and Furman [16], since the crystal radius of U^{5+} is closer to Zr^{4+}, the addition of Zr^{4+} tends to oxidize U^{4+} to U^{5+}, giving lower $\Delta\overline{G}_{O_2}$.

2.2. Metals having both +4 and +3 valence states

Stoichiometric solid solutions $M_yU_{1-y}O_{2.00}$ (M = Pu and Ce) are known to form for all y values between 0 and 1. The hypostoichiometric solid solution exists until all Pu (or Ce) ions are reduced to Pu^{3+} (or Ce^{3+}) together with U^{4+} [17]. In this case, however, there are upper limits in the y value for solid solutions, viz. 0.58 at 500°C [18] and 0.20 at room temperature [19] for Pu, and 0.7 at 260°C and 0.2 at room temperature for Ce [20]. In hyperstoichiometric solid solutions all Pu (or Ce) ions are oxidized to Pu^{4+} (or Ce^{4+}) and the U ions are to some extent from +4 state. The maximum y values in this region of solid solutions are 0.30 for Pu [18] and 0.50 ($x \leq 0.18$) for Ce [21] at room temperature.

The oxygen potential in the hypostoichiometric region increases with increasing x value giving a steeper slope as the x value approaches close to $x = 0$. After the almost vertical increase at $x = 0$, the oxygen potential rather slowly increases with increasing x in the hyperstoichiometric region [22–24]. The $\Delta\overline{G}_{O_2}$ values for $M_yU_{1-y}O_{2+x}$ (M = Pu and Ce) of various y values are considered to be expressed by the mean Pu (or Ce) valence and the mean U valence in the hypo and hyperstoichiometric regions, respectively [25]. The higher $\Delta\overline{G}_{O_2}$ values of Ce solid solution in the hypostoichiometric region may be because CeO_{2+x} ($x < 0$) has higher $\Delta\overline{G}_{O_2}$ than PuO_{2+x} ($x < 0$) [17].

2.3. Metals having +3 valence state

In reducing atmospheres, the solubility of Sc^{3+} is as low as a few mol% at 1100–1550°C [26] due to its smallest crystal radius of 1.01 Å (CN = 8) [11] in trivalent rare-earth ions. However, the solubilities of the other rare-earth ions are higher than $y = 0.5$. The solubilities are still high in oxidizing atmospheres, giving hyper-stoichiometric solid solutions [27].

In an analogy to the crystal radius effect for M^{4+} ions, the M^{3+} solid solutions with smaller M^{3+} crystal radii are expected to show lower $\Delta\overline{G}_{O_2}$, though not experimentally ascertained. The oxygen potential versus x curves for Y [28], La [29], Pr [17], Nd [30,31], Eu [32] and Gd [33] solid solutions show a similar feature to those of Pu and Ce solid solutions. The addition of higher content of rare-earth metals causes higher oxygen potentials.

2.4. Metals having +2 valence state

The solid solutions with $y = 0.33$ have been prepared in relatively high oxygen pressures for Mg, Ca, Sr, Ba and Cd[34]. However, in strongly reducing atmospheres, the solubilities of these divalent metals in UO_2 are low. The solubilities of Sr and Ba are $y = 0.12$ [35] and 0.03 [36], respectively.

As a result of the low valency of the M metals, the solid solutions show considerably higher $\Delta\overline{G}_{O_2}$ values than the M^{3+} and M^{4+} solid solutions. It is characteristic of Mg [37] and Ca [38] solid solutions that the x value which gives the rapid change in $\Delta\overline{G}_{O_2}$ shifts from $x = 0$ for M^{4+} or M^{3+} solid solutions to $x < 0$. The oxygen potential data for Ba solid solution are not available. However, it has been reported that $Ba_{0.05}Y_{0.05}U_{0.9}O_{2+x}$[39] gives the steepest $\Delta\overline{G}_{O_2}$ change at $x = -0.083$. Since Y does not contribute to this shift [28], Ba also appears to be responsible for the $x < 0$ shift. Park and Olander [40] explained this phenomenon by the mass-action law calculation of the metal–vacancy complexes. The above shift was also resolved by a statistical treatment [41,42], assuming that one M^{2+} atom forms a complex with α U^{5+} ($1 < \alpha < 2$). Both these methods attain eventually the quite similar results, though in the statistical method much attention is paid to the entropy change.

3. Mg solid solution in low oxygen partial pressures

3.1. Phase relations

By virtue of a small neutron absorption cross section, Mg has been thought to be one of the promising addition metals to UO_2 fuel for better performance during irradiation up to high burn-ups. According to the irradiation test up to 28500 MW d/tU, fission gas release from the 5 mol% MgO doped fuel was reduced by a factor greater than 2.5 × in comparison with that from standard irradiated UO_2 [4]. However, for this solid solution there are some inconsistencies in the solubility of Mg under low oxygen pressures [4,43,44]. Our experimental results [45] showed that the solubility strongly depends on oxygen partial pressure, where the measurement of the phase separation was carried out by the X-ray diffraction analysis of precipitated MgO.

Table 1
Single phase regions of Mg solid solution

Y:	0.1				0.15			
$P(O_2)$ (atm):	10^{-6} atm	10^{-8}	10^{-10}	10^{-19} (H_2)	10^{-6}	10^{-8}	10^{-10}	10^{-19} (H_2)
a_0 (Å):	5.4274	5.4483	5.4524	5.4660	5.3916	5.4487	5.4563	5.4675
X-ray diffraction:	single phase	two phases with small amount of MgO	two phases with MgO	single phase	single phase	two phases with MgO	two phases with MgO	two phases with small amount of MgO
Frequency of MgO in TEM:	2/90 3/120	n.e. [a]	35/150 25/110	2/130 2/190	3/95 3/110	n.e. [a]	n.e. [a]	10/150 9/120

[a] n.e.: not examined.

The solubility of Mg at 1200°C was examined also by transmission electron microscope (TEM) observation for quenched samples. The above two methods gave a consistent result, which is shown in Table 1. The reaction was carried out in a flowing gas of H_2/CO_2 for 50–70 h. The $y = 0.1$ samples show two single phase regions of solid solution at $p_{O_2} = 10^{-6}$ and $\leq 10^{-19}$ atm, separated by a two-phase region of $p_{O_2} = 10^{-8}$–10^{-10} atm. It has been observed that the solid solution is in a single phase also at 10^{-15} atm [45]. This implies that Mg is soluble in UO_2 at least up to $y = 0.1$ for oxygen partial pressures below $p_{O_2} = 10^{-15}$ atm. The Mg concentration of $y = 0.15$ is beyond the solubility even at $p_{O_2} = 10^{-19}$ atm. The TEM observation revealed that the single phase corresponds to the frequency of $\sim 1/50$ or less for finding any MgO part in the particles. In the two-phase region of $y = 0.15$ and $p_{O_2} \leq 10^{-19}$ atm, this frequency increased to $\sim 3/50$. Closer discussion on the TEM result will be made in the succeeding paper.

From Table 1, it is seen that the FCC solid solution changes its lattice parameter with p_{O_2} in the two-phase region in contradiction to the thermodynamic prediction. This may be because the thermodynamic equilibrium is not attained for the reaction pro-ducts. The reaction rate is possibly extremely low in this range of p_{O_2} as has been encountered during the $\Delta\bar{G}_{O_2}$ measurements.

3.2. Density of the Mg solid solution

The density of the solid solution measured by the toluene displace method is shown in Fig. 1. The square and triangle marks express the data for $p_{O_2} = 10^{-15}$ and $\leq 10^{-19}$ atm, respectively. The solid and dotted lines show the theoretical change of the solid solution for $p_{O_2} = 10^{-15}$ and $\leq 10^{-19}$ atm, respectively. In the above theoretical curves those which decrease and increase with increasing y value indicate substitutional and interstitial solid solutions, respectively. It is noteworthy that the U valencies in the solid solutions with various y values in the figure are all close to +4. The dash–dotted line shows the theoretical change if the product is a mixture of MgO and UO_2. The observed densities for $UO_{2.000}$ ($y = 0$) are lower than the theoretical value by ~ 0.08 g/cm^3, which is considered to be ascribed to the closed pores in the particles and this effect is assumed to exist for solid solutions. After the correction for this lowering, the observed densities become significantly higher than the theoretical line for the mixtures, confirming that the products are not the mixtures.

Since the observed densities are between the substitutional and interstitial theoretical lines, the solid solution is considered to consist of the Mg atoms which are partly in the substitutional position (4a in space group Fm3m) and partly in the interstitial position (4b), as expressed by $(Mg_{y_1}U_{1-y_1})\{Mg_{y_2}\}O_{2+y_2-y_1}$ where y_1 and y_2 are the substitutional and interstitial Mg atoms, respectively. The calculated interstitial atom ratio, $y_2/(y_1 + y_2)$, increases from ~ 0.2 for $y = 0.05$ to 0.4 for $y = 0.1$ in $p_{O_2} = 10^{-15}$ atm pressure, but it remains almost unchanged at ~ 0.6 in $\leq 10^{-19}$ atm.

3.3. Statistical calculation

For simplicity, let us consider that MgO dissolves into stoichiometric UO_2 forming solid solution. The Mg^{2+} ions occupy both the substitutional and interstitial sites. This reaction is described as

$$z\mathrm{MgO} + \mathrm{UO_2} = \frac{1}{1-y_1}\left(\mathrm{Mg}_{y_1}\mathrm{U}_{1-y_1}\right)\left\{\mathrm{Mg}_{y_2}\right\}\mathrm{O}_{2+y_2-y_1}, \tag{1}$$

where $z = (y_1 + y_2)/(1 - y_1)$. If we put $x = y_2 - y_1$,

$$y_1 = \frac{z-x}{z+2} \quad \text{and} \quad y_2 = \frac{xz+x+z}{z+2}.$$

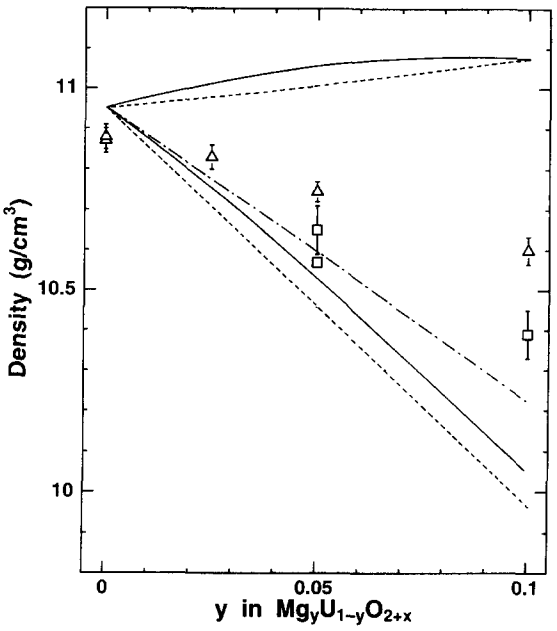

Fig. 1. Variation of density with y of $M_yU_{1-y}O_{2+x}$ ($x \gtreqless 0$) expression. (□) $p_{O_2} = 10^{-15}$ atm, (△) $p_{O_2} \leq 10^{-19}$ atm. ————: Theoretical lines for $p_{O_2} = 10^{-15}$ atm. - - -: Theoretical lines for $p_{O_2} \leq 10^{-19}$ atm. – · –: Theoretical line for the mixture of MgO and UO_2.

Then, the number of the 4a metal site in the solid solution is $(z+2)N/(x+2)$, where N is Avogadro's number. The number of ways of arranging Mg^{2+} and U^{4+} ions over the lattice sites is

$$W_1 = \frac{(\{(z+2)/(x+2)\}N)!}{(\{(z+2)/(x+2)\}N\{(z-x)/(z+2)\})!(\{(z+2)/(x+2)\}N\{(x+2)/(z+2)\})!}. \tag{2}$$

Since the number of the oxygen atom site in the solid solution is $(z+2)2N/(x+2)$ from Eq. (1), the number of ways of arranging O^{2-} ions and oxygen vacancies over the anion lattice sites is

$$W_2 = \frac{(\{(z+2)/(x+2)\}2N)!}{(\{(z+2)/(x+2)\}2Nx/2!(\{(z+2)/(x+2)\}2N(2-x)/2)!}. \tag{3}$$

The number of interstitial sites (4b site) is $(z+2)N/(x+2)$. Therefore, the number of ways of arranging the interstitial Mg^{2+} ions over these lattice sites becomes

$$W_3 = \frac{(\{(z+2)/(x+2)\}N)!}{(\{(z+2)/(x+2)\}N\{(x+z+xz)/(z+2)\})!(\{(z+2)/(x+2)\}N\{(2-x-xz)/(z+2)\})!}. \tag{4}$$

The partial molar entropy of oxygen per mole of O_2, $\Delta\bar{S}_{O_2}$, is given as

$$\Delta\bar{S}_{O_2} = 2kN\frac{\partial \ln(W_1W_2W_3)}{\partial(xN)} + Q = 2R\frac{2+z}{(2+x)^2}\ln\frac{(-x+z)(2-x)^4(2-x-xz)^2}{4x^2(2+z)^2(x+z+xz)} + Q, \tag{5}$$

where R is the gas constant and Q is the factor which includes the vibrational entropy of the crystal and the standard entropy of oxygen. The Q value has been insensitive to the compositional change of the solid solution [46]. Using Eq. (5), the oxygen potential is written as

$$\Delta\bar{G}_{O_2} = \Delta\bar{H}_{O_2} - 2RT\frac{2+z}{(2-x)^2}\ln\frac{(X+z)(2+X)^4(2+X+Xz)^2}{4X^2(2+z)^2(-X+z-Xz)} - QT, \tag{6}$$

where x is replaced by $X = -x = y_1 - y_2$ which is assumed to be positive in the low p_{O_2} region of the solid solution.

In the above equation, the composition dependence of the $\Delta\bar{H}_{O_2}$ and QT terms is disregarded since the changes of these terms are supposed to be small in the solid solution. From Eq. (6) it is seen that $\Delta\bar{G}_{O_2}$ decreases toward $-\infty$ at two cases of

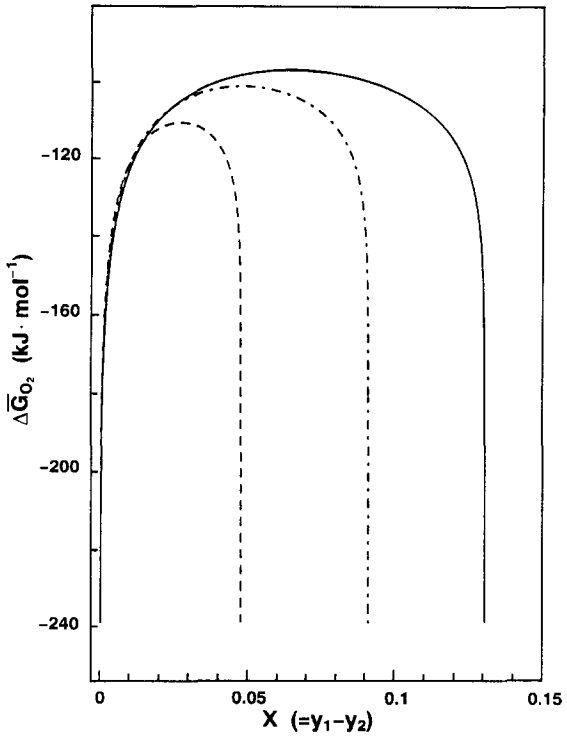

Fig. 2. Calculated contribution of configurational entropy to $\Delta\overline{G}_{O_2}$ (at 1000°C) as a function of X. ——: $z = 0.05$; ---: $z = 0.1$; ——————: $z = 0.15$. The value, z, means the MgO concentration when the solid solution is considered to be formed by zMgO + UO_2.

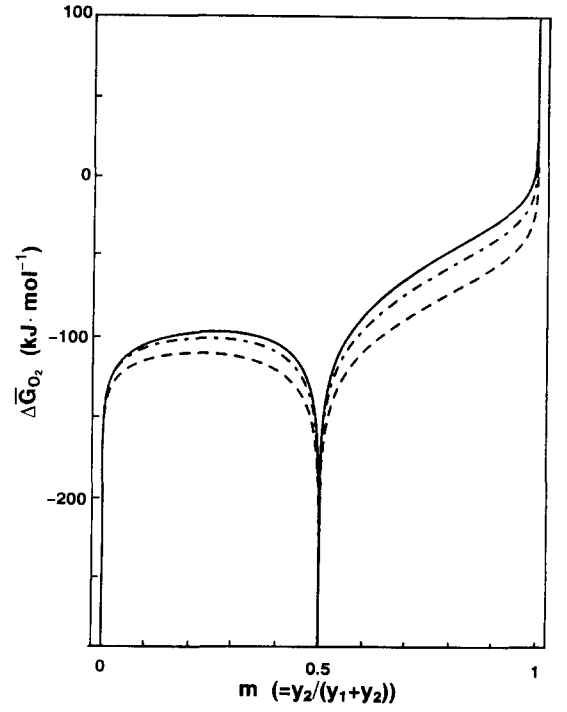

Fig. 3. Calculated $\Delta\overline{G}_{O_2}$ change (at 1000°C) as a function of interstitial Mg fraction, m. ---: $z = 0.05$; – · –: $z = 0.1$; ——————: $z = 0.15$.

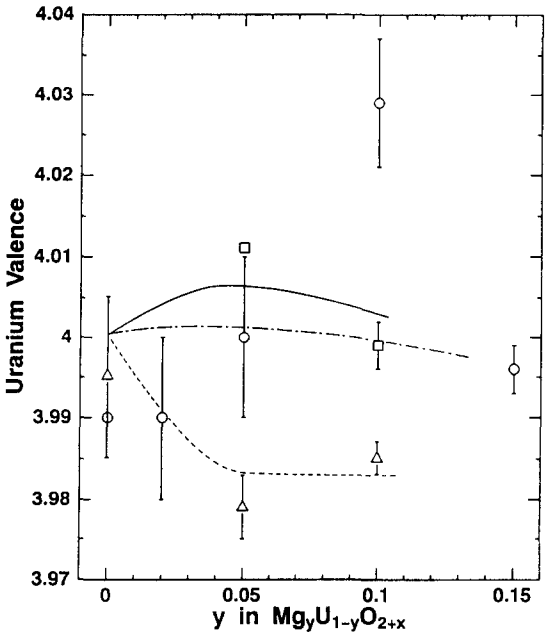

Fig. 4. Mean valence of U in $M_yU_{1-y}O_{2+x}$ ($x \gtreqless 0$) plotted against y value [45]. (□) $p_{O_2} = 10^{-15}$ atm. (○ and △) Two runs under $p_{O_2} \leq 10^{-19}$ atm.

$X = 0$ and $X = z/(1+z)$. When $X = 0$, y_1 is equal to y_2. The concentrations of substitutional and interstitial Mg ions are the same. On the other hand when $X = z/(1+z)$, all Mg ions enter the substitutional sites. Fig. 2 shows the contribution of the above configurational entropy to $\Delta\bar{G}_{O_2}$ as a function of X. The broken, dash–dotted and solid lines indicate the $\Delta\bar{G}_{O_2}$ change for $z = 0.05$, 0.1 and 0.15, respectively. The $\Delta\bar{G}_{O_2}$ curves are seen to decrease sharply at $X = 0$ and $z/(1+z)$. In Fig. 3, this relation is replotted as a function of interstitial Mg atom ratio, m. Fig. 3 depicts that $\Delta\bar{G}_{O_2}$ increases monotonically above 50% interstitial Mg.

It should be noted that the $\Delta\bar{G}_{O_2}$ variation in Fig. 3 was obtained on the assumption that the solid solution is composed of MgO and stoichiometric UO_2, i.e., the U valency in the solid solution is +4. Fig. 4 shows the U valence determined by chemical analysis [45]. If the solid solution is formed by z mol MgO and 1 mol hypostoichiometric UO_{2-a}, the formula will be

$$\frac{z-a+2}{x+2}\left(\mathrm{Mg}_{\frac{z-x-a}{z-a+2}}\mathrm{U}_{\frac{x+2}{z-a+2}}\right)\left\{\mathrm{Mg}_{\frac{xz+x+z+a}{z-a+2}}\right\}\mathrm{O}_{2+x},$$

where we put here $x = y_2 - y_1 - a(1-y_1)$. The similar calculation as above leads to give another expression of $\Delta\bar{G}_{O_2}$ as

$$\Delta\bar{G}_{O_2} = \Delta\bar{H}_{O_2} - 2RT\frac{2-a+z}{(2-X)^2}\ln\frac{(-a+X+z)(2+X)^4(2-2a+X+Xz)^2}{4X^2(2-a+z)^2(a-X+z-Xz)} - QT, \tag{7}$$

where $X = -x$. The above equation shows that $\Delta\bar{G}_{O_2}$ decreases toward $-\infty$ at $X = 0$ or $(a-X+z-Xz) = 0$. At the former X value, the interstitial Mg ratio, m, is

$$m = \frac{y_2}{y_1+y_2} = \frac{1}{2} + \frac{a}{2z}. \tag{8}$$

That is to say, if $m = 0.6$ as obtained experimentally under $p_{O_2} \leq 10^{-19}$ atm, $a = 0.01$ ($UO_{1.99}$) for $z = 0.05$ and $a = 0.02$ ($UO_{1.98}$) for $z = 0.1$. The U valencies for these Mg concentrations are +3.98 and +3.96, respectively, in good agreement with the chemically determined U valencies in Fig. 4. Eq. (8) shows that the ratio of interstitial Mg atoms becomes $> 1/2$ by the slight reduction of U lower than +4. The reason that the substitutional solid solution ($(a-X+z-Xz) = 0$) does not exist in very low p_{O_2} may be because the crystal is unstable, with regard to $\Delta\bar{H}_{O_2}$, to the high concentration of oxygen vacancies needed for the formation of the substitutional Mg solid solution.

4. Conclusions

First, a short review is given on the phase relations and oxygen potentials of $M_yU_{1-y}O_{2+x}$ ($M = M^{4+}$, M^{4+-3+}, M^{3+} and M^{2+}) solid solutions as classified by the valence of the doped M metals. (1) M^{4+} metals: ThO_2 forms a continuous solid solution with stoichiometric UO_2, but the solubility of ZrO_2 in UO_2 is low. $\Delta\overline{G}_{O_2}$ of $Th_yU_{1-y}O_{2+x}$ ($x \geq 0$) increases with increasing y value, whilst that of $Zr_yU_{1-y}O_{2+x}$ decreases possibly caused by smaller crystal radius of Zr^{4+}. (2) M^{4+-3+} metals: Although stoichiometric solid solutions $M_yU_{1-y}O_{2.00}$ ($M = Pu$ and Ce) are formed for all y values between 0 and 1, the solubility of the M metals decreases with oxygen non-stoichiometry. $\Delta\overline{G}_{O_2}$ increases with an increase in y of $M_yU_{1-y}O_{2+x}$ of which the steepest change takes place at $x = 0$. (3) M^{3+} metals: The solubilities of trivalent rare-earth ions in UO_{2+x} are higher than $y = 0.5$ except for Sc^{3+}. The effect of M^{3+} metals on $\Delta\overline{G}_{O_2}$ is similar to that of M^{4+-3+} metals. (4) M^{2+} metals: The solid solutions with $y = 0.33$ have been prepared in relatively high oxygen pressures for Mg, Ca, Sr, Ba and Cd. However, the solubilities are much less in low oxygen pressures, and that for Mg is not in good agreement in the reports. The x values of $M_yU_{1-y}O_{2+x}$, which give the steepest change in $\Delta\overline{G}_{O_2}$, are shifted to $x < 0$, in contrast to the cases of M^{4+}, M^{4+-3+} and M^{3+} metals.

In the second part, our thermodynamic study on the Mg solid solution in low oxygen pressures is described. The solubility of Mg in UO_2 at 1200°C under $p_{O_2} \leq 10^{-15}$ atm is over $y = 0.1$. Above $p_{O_2} = 10^{-6}$ atm, the maximum y value is larger approaching 0.33, but between $p_{O_2} = \sim 10^{-8}$ and $\sim 10^{-10}$ atm there lies an insoluble region. Density measurements showed that the Mg atoms should occupy partly the interstitial sites (possibly 4b of Fm3m). The ratio, m, of the interstitial Mg atoms to the total Mg atoms is ~ 0.2 for $y = 0.05$ or 0.4 for $y = 0.1$ at $p_{O_2} = 10^{-15}$ atm, while it increases to ~ 0.6 at $\leq 10^{-19}$ atm. The stability of occupation of the Mg atoms in the interstitial sites was studied by statistically calculating $\Delta\overline{S}_{O_2}$ and considering its effect on $\Delta\overline{G}_{O_2}$. It was shown that the calculated $\Delta\overline{G}_{O_2}$ values are very low at $m = 0$ (100% substitutional) and 0.5 (50% substitutional and 50% interstitial). Calculation also revealed that if the solid solution is formed with hypostoichiometric UO_{2-a}, the m value of 0.5 could shift to > 0.5; e.g., if $a = 0.01$ ($UO_{1.99}$, U valency +3.98) for 5% Mg solid solution, m becomes 0.6.

References

[1] F. Schleifer, A. Naoumidis, H. Nickel, J. Nucl. Mater. 115 (1985) 143.
[2] K. Une, M. Oguma, J. Nucl. Sci. Technol. 20 (1983) 844.
[3] H. Holleck, W. Wagner, in: Thermodynamics of Nuclear Materials, Proc. Symp. 1967 (IAEA, Vienna, 1968) p. 667.
[4] P.T. Sawbridge, C. Baker, R.M. Cornell, K.W. Jones, D. Reed, J.B. Ainscough, J. Nucl. Mater. 95 (1980) 119.
[5] K.C. Radford, J.M. Pope, J. Nucl. Mater. 116 (1983) 305.
[6] J.C. Killeen, J. Nucl. Mater. 58 (1975) 39.
[7] J.C. Killeen, J. Nucl. Mater. 88 (1980) 177.
[8] J.B. Ainscough, F. Rigby, S.C. Osborn, J. Nucl. Mater. 52 (1974) 191.
[9] M. Hirai, J. Nucl. Mater. 173 (1990) 247.
[10] S.D. Preston, C. Barrett, P. Fassina, K.C. Mills, N. Zaghini, High Temp. High Press. 21 (1989) 287.
[11] R.D. Shannon, Acta Crystallogr. A32 (1976) 751.
[12] K. Une, M. Oguma, J. Am. Ceram. Soc. 66 (1983) c–179.
[13] S. Aronson, J.C. Clayton, J. Chem. Phys. 35 (1961) 1055.
[14] R. Paul, C. Keller, J. Nucl. Mater. 41 (1971) 133.
[15] S. Aronson, J.C. Clayton, J. Chem. Phys. 32 (1960) 749.
[16] M. Hoch, F.J. Furman, in: Thermodynamics, Proc. Symp. 1965, Vol. 2 (IAEA, Vienna, 1966) p. 517.
[17] T. Fujino, C. Miyake, in: Handbook on the Physics and Chemistry of the Actinides, Vol. 6, ed. A.J. Freeman and C. Keller (North-Holland, Amsterdam, 1991) p. 173.
[18] T.L. Markin, R.S. Street, J. Inorg. Nucl. Chem. 29 (1967) 2265.
[19] C. Sari, U. Benedict, H. Blank, J. Nucl. Mater. 35 (1967) 267.
[20] R. Lorenzelli, B. Touzelin, J. Nucl. Mater. 95 (1980) 290.
[21] T.L. Markin, R.S. Street, E.C. Crouch, J. Inorg. Nucl. Chem. 32 (1970) 59.
[22] J. Edwards, R.N. Wood, G.R. Chilton, J. Nucl. Mater. 130 (1985) 505.
[23] R.E. Woodley, J. Nucl. Mater. 96 (1981) 5.
[24] G.R. Chilton, J. Edwards, in: Thermodynamics of Nuclear Materials, Proc. Symp. 1979, Vol. 1 (IAEA, Vienna, 1980) p. 357.
[25] T.L. Markin, E.J. McIver, in: Plutonium 1965, Proc. 3rd Int. Conf. on Plutonium, 1965, ed. A.E. Kay and M.B. Waldron (Barnes and Noble, London, 1967) p. 845.
[26] C. Keller, U. Berndt, M. Debbabi, H. Engerer, J. Nucl. Mater. 42 (1972) 23.
[27] H.G. Diehl, C. Keller, J. Solid State Chem. 3 (1971) 621.
[28] K. Hagemark, M. Broli, J. Am. Ceram. Soc. 50 (1967) 563.

[29] T. Matsui, K. Naito, J. Nucl. Mater. 138 (1986) 19.
[30] K. Une, M. Oguma, J. Nucl. Mater. 118 (1983) 189.
[31] J.F. Wadier, Report CEA-R-4507, 1973.
[32] T. Fujino, K. Ouchi, Y. Mozumi, R. Ueda, H. Tagawa, J. Nucl. Mater. 174 (1990) 92.
[33] T.B. Lindemer, A.L. Sutton Jr., J. Am. Ceram. Soc. 71 (1988) 553.
[34] H.R. Hoekstra, S. Siegel, Proc. Int. Conf. Peaceful Uses of Atomic Energy, Vol. 7, Geneva, 1955, p. 394.
[35] E.J. McIver, Report AERE-M-1612, 1966.
[36] H. Kleykamp, J. Nucl. Mater. 131 (1985) 221.
[37] J. Tateno, T. Fujino, H. Tagawa, J. Solid State Chem. 30 (1979) 265.
[38] T. Yamashita, to be published.
[39] T. Fujino, T. Yamashita, K. Ouchi, J. Nucl. Mater. 183 (1991) 46.
[40] K. Park, D.R. Olander, J. Nucl. Mater. 187 (1992) 89.
[41] T. Fujino, N. Sato, J. Nucl. Mater. 189 (1992) 103.
[42] T. Fujino, N. Sato, K. Yamada, J. Nucl. Mater. 223 (1995) 6.
[43] T. Fujino, J. Tateno, H. Tagawa, J. Solid State Chem. 24 (1978) 11.
[44] J.S. Anderson, K.D.B. Johnson, J. Chem. Soc. (1953) 1731.
[45] T. Fujino, S. Nakama, N. Sato, K. Yamada, K. Fukuda, H. Serizawa, T. Shiratori, J. Nucl. Mater. in press
[46] E. Stadlbauer, U. Wichmann, U. Lott, C. Keller, J. Solid State Chem. 10 (1974) 341.